EPJ Web of Conferences **208**, 14008 (2019) https://doi.org/10.1051/epjconf/201920814008
ISVHECRI 2018

On the origin of the TeV gamma-ray emission from Cygnus X-3

V.G. Sinitsyna[1,*], V.Y. Sinitsyna[1]

[1]P. N. Lebedev Physical Institute, Russian Academy of Sciences

Abstract. Cygnus X-3 binary system is a famous object studied over the wide range of electromagnetic spectrum. Early detections of ultra-high energy gamma-rays from Cygnus X-3 by Kiel, Havera Park and then by Akeno triggered the construction of several large air shower detectors. Also, Cygnus X-3 has been proposed to be one of the most powerful sources of charged cosmic ray particles in the Galaxy. The results of twenty-year observations of the Cyg X-3 binary at energies 800 GeV - 85 TeV are presented with images, spectra during periods of flaring activity and at low flux periods. The correlation of TeV flux increases with flaring activity at the lower energy range of X-ray and radio emission from the relativistic jets of Cygnus X-3 is found as well as 4.8-hour orbital modulation of TeV γ-ray intensity. Detected modulation of TeV γ-ray emission with orbit and important characteristics of Cyg X-3 such as the high luminosity of the companion star and the close orbit leads to an efficient generation of γ-ray emission through inverse Compton scattering in this object. The different type variability of very high-energy γ-emission and correlation of radiation activity in the wide energy range can provide essential information on the mechanism of particle production up to very high energies.

1 Introduction

Relativistic objects in the Galaxy at very high energies have been searched for in the SHALON experiment from the very beginning of its operation [1–5]. In 1995 the observations by the SHALON mirror Cherenkov telescope revealed a new Galactic source of γ-ray emission at very high energies $E > 800$ GeV [4]. The position of the emission source recorded in our experiment coincides in its coordinates with the X-ray binary system Cyg X-3 [4, 5] which has been systematically observed by the SHALON telescope since 1995 up until now [4–6].

Gamma-ray emission from Cyg X-3 was detected by the SHALON telescope at energies above 800 GeV at a 34.1σ level determined using Eq. (17) from [7]. The mean integral flux at energies above 800 GeV for Cyg X-3 is $I_{CygX-3}(> E_\gamma) = (6.8 \pm 0.4) \times 10^{-13}$ cm^{-2} s^{-1}. The differential spectrum of Cyg X-3 was obtained by SHALON in the energy range 800 GeV - 100 TeV and is presented in Fig. 1 together with the upper limits by the VERITAS [8] and MAGIC [9] experiments.

2 Cyg X-3 Orbital period

To reliably identify the detected source with Cyg X-3, we performed an analysis aimed at searching for the orbital period of 4.8 h that is a signature of Cyg X-3. The light curve for the source detected by SHALON was folded and includes events that passed the selection criteria and that were used to construct its spectrum (Fig. 1). We used the parabolic ephemerides of Cyg X-3 from [10, 11] with an orbital period of 0.1996843 day and an epoch of the minimum X-ray flux JD 2454857,193 [11]. In papers [12–14]

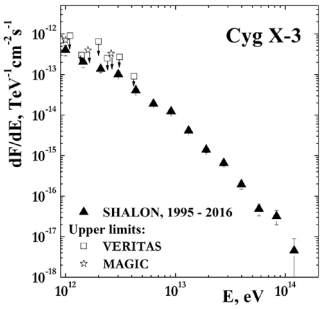

Figure 1. Differential spectrum of Cyg X-3 from the SHALON data compared with the VERITAS [8] and MAGIC [9] data.

it was shown that the orbital period of Cyg X-3 slowly changes. For the quadratic ephemerides used, the time derivative of the period is 6.48×10^{-10}, i.e., the orbit of Cyg X-3 changes on a scale of 1.18×10^{-6} yr^{-1}. As a result, we folded all the events detected as γ-rays with energies > 800 GeV with the given period of the source (0.1996843 day) into the light curves with a length of one period divided into 15 intervals. The event arrival time was corrected for the Earth's orbital motion. The observation time of Cyg X-3 for each individual interval of the light curve varies significantly. So, each event was taken with the corresponding weight that took into account the observation time in this interval. The derived light curve has a pseudo-sinusoidal shape with a rise followed by a decay, and a period of 4.79143 h characteristic for the orbital motion of the binary system Cyg X-3 (Fig. 2, left).

It was found [15], that the folded light curves in the energy ranges of 800 GeV - 100 TeV, 100 MeV - 100 GeV, 20 - 100 keV and 2 - 15 keV have the same asymmetric shape with a slow rise and a faster decay. In contrast to the X-ray light curves, ones at high and very high ener-

*e-mail: sinits@sci.lebedev.ru

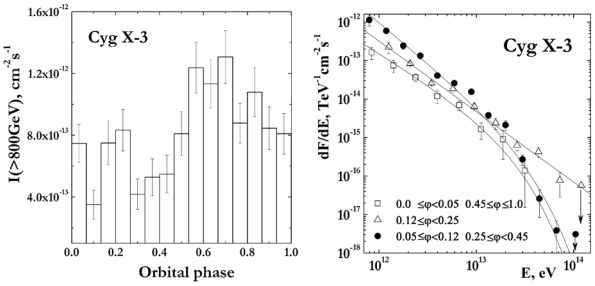

Figure 2. left: The SHALON light curve of Cyg X-3 folded with the orbital period of 4.8 h. **right:** The differential γ-ray spectra for Cyg X-3 at very high energies in different intervals of orbital modulation. The lines represent the fit to each spectrum.

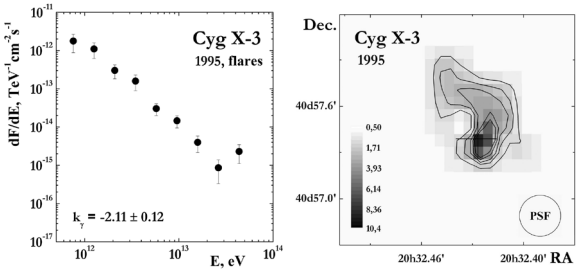

Figure 3. Differential spectrum of the γ-ray emission from Cyg X-3 and image of Cyg X-3 at energies > 0.8 TeV during the flux increase in 1995.

gies (see [15]) have an additional local maximum in the region of the global minimum (phases ∼0.3 and ∼0.2 for the Fermi LAT and SHALON experiments, respectively). In addition, there is a phase shift of the minimum in the light curves at different energies. For example, the flux minimum from the SHALON data lags behind the X-ray flux minimum by ∼0.2 in phase and leads the flux minimum measured by Fermi LAT by ∼0.15. In [16] it was shown that there is a ∼20 min time delay between the soft XTE/ASM (2 - 12 keV) and hard OSSE (44 - 130 keV) X-ray light curves. Subsequently, a slight phase time delay of (5.5 ± 8.6)min between the hard 40 - 100 keV (ISGRI) and soft 15 - 40 keV (IBIS) X-ray fluxes was reported [17].

3 Phase-resolved energy spectra

The determination of the energy spectrum of TeV γ-ray emission is important for understanding the mechanism of radiation production. For binaries the phase resolved spectra can also point out the site of origin. Differential spectra for three intervals of orbital phase were extracted.

The interval with maximum flux corresponding to inferior conjunction at phase $0.0 \leq \phi < 0.05$; $0.45 \leq \phi < 1.0$; The γ-ray energy spectrum is well described by a relatively soft power law with an exponential cutoff:

$(1.2 \pm 0.1) \times 10^{-12} \times E^{-2.05\pm0.10} \times exp(-E/20\ \mathrm{TeV})$

The interval with additional maximum at the phase of superior conjunction at phase $0.12 \leq \phi < 0.25$; Here the γ-ray energy spectrum is described by a hard power law:

$(0.51 \pm 0.09) \times 10^{-12} \times (E/1\mathrm{TeV})^{-1.83\pm0.12}$

The interval with minimum flux corresponding to superior conjunction at phase $0.05 \leq \phi < 0.12$; $0.25 \leq \phi \leq 0.45$; The γ-ray energy spectrum is described by a hard power law with an exponential cutoff:

$(0.35 \pm 0.08) \times 10^{-12} \times E^{-1.65\pm0.11} \times exp(-E_\gamma/14.5\ \mathrm{TeV})$

4 The flaring activity of Cyg X-3

The periods of a high intensity and flares in Cyg X- 3 at energies > 800 GeV were found to have occurred at a certain relationship between the radio and X-ray activities [15].

Increased TeV γ-ray flux was observed in the period of low radio flux densities during the fall to ∼10 - 20 mJy and 4 - 7 days before its rise to ∼300 - 600 mJy, the so-called minor flare. Also, a high TeV flux is detected within 1 - 7 days before the major flare with a flux density of 1000 - 9000 mJy in the period of high soft X-ray and low hard X-ray fluxes. An increase of the very high energy gamma-ray flux during a high activity in soft X-rays and a low activity in hard X-rays within 2 - 6 days after minor radio flares was also observed.

Table 1. Test of the correlation between the data obtained in the SHALON observations of Cyg X-3 and at low energies.

Source state	r_s	p
HTeV vs SXR	0.81	1.7×10^{-5}
HTeV vs HXR	-0.61	8.9×10^{-3}
LTeV vs SXR	0.83	1.8×10^{-7}
LTeV vs HXR	-0.90	1.5×10^{-7}
HTeV vs Radio	0.87	7.2×10^{-3}

When analyzing the SHALON light curve [15], it was noted that the periods of a low source intensity at very high energies occurred in the intervals of low radio and soft X-ray activities, while the hard X-ray fluxes are high.

To test the existence of correlations, we calculated the Spearman rank correlation coefficient (r_s) and the probability of its absence (p) to estimate the significance of the correlation. The following states in different energy ranges were extracted to reveal the correlation:

LTeV - low integral fluxes at energies > 0.8 TeV with $I_{LTeV}(> 0.8\ \mathrm{TeV}) < 4.5 \times 10^{-13}\ \mathrm{cm}^{-2}\ \mathrm{s}^{-1}$,

HTeV - high gamma-ray fluxes at $E > 0.8$ TeV with $I_{HTeV}(> 0.8\ \mathrm{TeV}) > 1.5 \times 10^{-12}\ \mathrm{cm}^{-2}\ \mathrm{s}^{-1}$;

SXR - soft X-ray fluxes (RXTE/ASM from 1996 and MAXI from 2012) corresponding in time to the SHALON data at TeV energies;

and HXR - hard X-ray fluxes (Swift BAT from 2005) also corresponding in time to the SHALON observations.

The correlation coefficient of the fluxes at very high energies HTeV with the radio emission (Radio) from the RT/AMI data (from 1995) during flares with a flux density > 300 mJy was calculated as a function of the time shift dT. The maximum value of r_s is given in Table 1 and is reached at $dT = 7 \pm 2$ days. The results of testing the correlation for the described relationships between the states at very high energies and in the soft X-ray, hard X-ray, and radio bands are presented in Table 1. The SHALON data showed that an increased activity of Cyg X-3 at energies above 800 GeV was observed, on average, within 6 - 8 days before its radio flares.The uncertainty in the shift arises from the gaps in the observations at very high energies by the technique of mirror Cherenkov telescopes. A correlation between the very high energy γ-ray flux and the soft X-ray flux is also traced over the entire period of

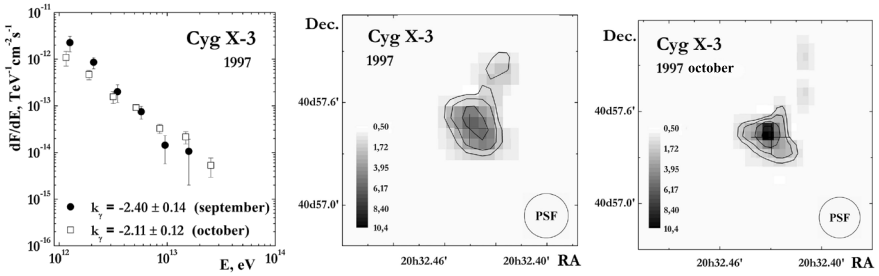

Figure 4. Differential spectra of the γ-ray emission from Cyg X-3 during its flux increase in 1997. Images of Cyg X-3 at energies > 0.8 TeV during its flux increase in September and October of 1997.

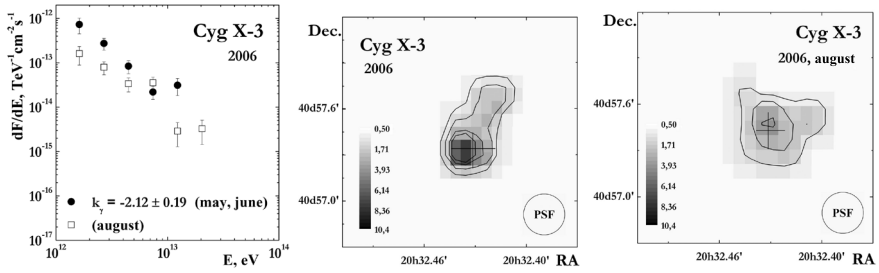

Figure 5. Differential spectra of the γ-ray emission from CygX-3 during its flux increase in May 2006 and flux decrease in August. Images of Cyg X-3 at energies > 0.8 TeV during its flux increase in May 2006 and flux decrease in August 2006.

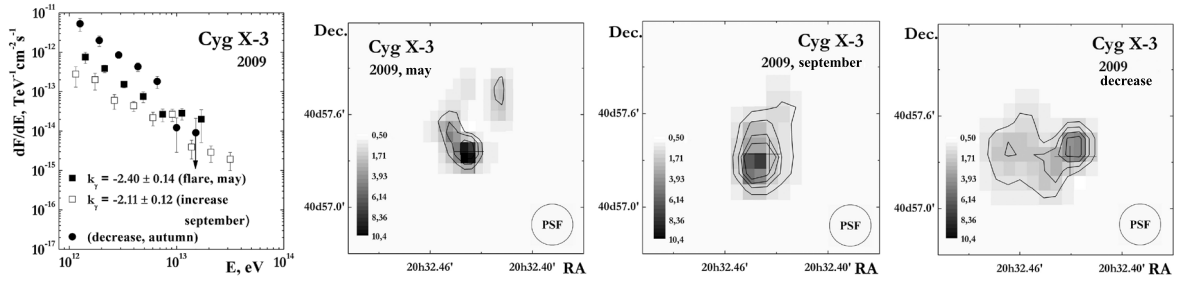

Figure 6. Differential spectra of the γ-ray emission from Cyg X-3 during the flux increases and decrease in 2009. Images of Cyg X-3 at energies > 0.8 TeV during its flux increase in May 2009, increase in September 2009 and flux decrease in October-November 2009.

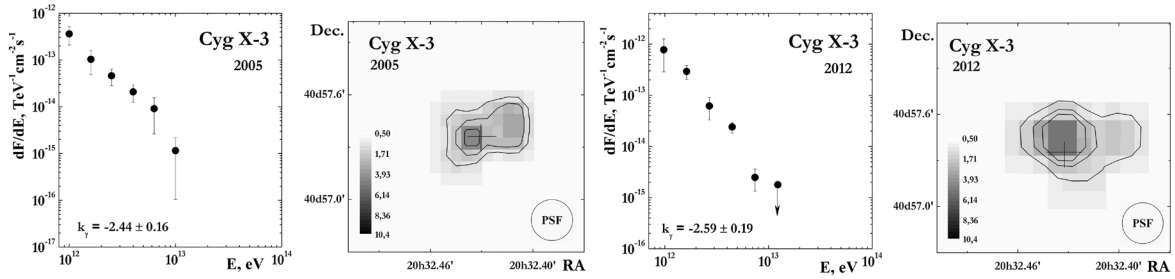

Figure 7. Differential spectra and images of the γ-ray emission of Cyg X-3 at $E > 0.8$ TeV in the quiescent periods of 2005 and 2012.

SHALON observations, while there is an anticorrelation with the hard X-ray flux.

Figs. 3,4,5,6 present the spectra and images of Cyg X-3 at TeV energies from the SHALON observations in different periods of activity. The intensity range in the images is presented on the same scale and the color scale is in units of the excess above the minimum detectable signal. The black circles in the figures indicate the PSF of the experiment. The PSF size after the second reconstruction step [18, 19] is from 12′′ to 20′′ in the case of a source with a hard spectrum with Γ_{diff} ∼2.1 corresponding to Cyg X-3. It was found [15], that in the periods of a high activity before minor and major radio flares at energies > 800 GeV, the emission from the source is characterized by a hard power-law spectrum with an index $\Gamma_{diff} \sim 2.1$ (Figs. 3,4,5,6); it is detected from a ∼ 20′′ region around Cyg X-3 with the presence of jets. In quiescence the emission originates from ∼ 40′′ region and its spectrum is described by a softer power law with an index $\Gamma_{diff} \sim 2.5$ (Fig.7).

In [20] the behavior of Cyg X-3 in the radio and X-ray bands was analyzed and revealed six states, depending on the ratio of the intensities in these ranges and the spectral characteristics in the X-ray energy band (see Fig. 8).

According to this diagram the behavior of Cyg X-3, the flare of Cyg X-3 at very high energies (Fig. 6, May) with a soft power-law spectrum refers to region 1 in Fig. 8 corresponding to the hypersoft state. The high intensity of the γ-ray emission characterized by a hard power-law spectrum (Fig. 6, September) corresponds to region 4 in Fig. 8 at the boundary of the transition to region 5. The state of Cyg X-3 presented in Figs. 3 and 4 probably also refers to this region, although there are no complete data on the behavior of the source at X-ray energies. The low-intensity emission at TeV energies with a hard spectrum (Fig.6, De-

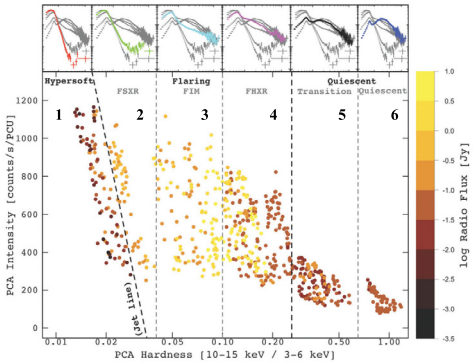

Figure 8. Diagram of states adopted from [20]

crease) corresponds to region 5 in Fig. 8. The increase in the intensity of emission with a hard spectrum observed in 2006 (Fig.5) corresponds to region 2 on the diagram. The quiescent state at very high energies (Fig. 7) refers to region 6 in Fig. 8. As a result, the diagram of states from [20] can be supplemented with information about the behavior of Cyg X-3 at very high energies, namely with the data on the intensity and spectral characteristics in the observation intervals under discussion.

5 The origin of TeV emission from Cyg X-3

The generation of very high energy γ-rays requires the presence of particles accelerated to energies higher than TeV and a target containing photons and/or matter of sufficient density. As Cyg X-3 is a microquasar-type object particle acceleration could take place both directly inside and along the jet up to parsec distances and in the regions close to the jet ends due to the interaction with the external environment [21]. The scenario based on the acceleration of particles at the shock waves produced by the interaction of a jet with matter inside the binary system is also possible. Presently, both leptonic and hadronic origins of the primary particles responsible for the very high energy γ-ray emission in these objects are considered. It was noted that the flaring activity of Cyg X-3 at energies above 0.8 TeV occur close, within 6 - 8 days, to minor and major radio flares. Such a behavior could be associated with powerful mass ejections from the central regions around the black hole accompanied by the propagation of relativistic shock waves where relativistic electrons and magnetic fields are generated rapidly and efficiently. The observed delay between the γ-ray and radio flares suggests that it occurs at distances of ~150 mas from the system. Indeed, during radio flares the emission is observed at distances of tens of milli-arc-seconds from the central object and a jet propagation velocity up to 0.6 - 0.8 s [22]. At the same time, the detected orbital modulation of the very high energy emission suggests that the size of the emitting region is smaller than the size of the orbit and is variously estimated to be $(2-3)\times10^{11}$ cm [23]. Inverse Compton (IC) scattering of photons in the wind from the Wolf-Rayet companion star by very high energy electrons is a natural candidate for very high energies.

The IC scattering directly produces a modulation of the γ-ray flux due to the orbital motion. The maximum corresponds to the orbital phase when the photons from the Wolf-Rayet star are rescattered toward the observer (Fig. 2). The connection found between the TeV γ-ray emission and radio flares suggests that high-energy electrons are located in relativistic jets. Important characteristics of Cyg X-3 are the high luminosity of the companion star and the close orbit, which, as shown in [24], leads to an efficient generation of γ-ray emission through the IC scattering in this object. An unusual property of the binary system Cyg X-3 is a strong wind from the companion star with a velocity of ~1000 km s^{-1} and a high density reaching 10^{13} cm^3 [23]. The combination of these characteristics could lead to the generation of very high energy γ-ray emission if cosmic rays are also accelerated in the source and then interact with nuclei in the stellar wind. The detection of γ-ray emission in the interval of orbital phases corresponding to superior conjunction (the additional maximum, Fig. 2) at very high energies in a wide range, from 800 GeV to 100 TeV, with a hard spectrum shows no cutoff points to the hadronic origin of the detected photons, with the proton spectrum extending to ~ 10^{15} eV [25]. Probably, particle acceleration may occur due to the interaction of the jet with the matter of the Wolf-Rayet star when the central object of the binary system is eclipsed by the star.

References

[1] S.I. Nikolsky, V.G. Sinitsyna, in Proc. of Int. Workshop of VHE Gamma-ray Astronomy, 1989, Ed. A. A. Stepanian
[2] S.I. Nikolskyi, V.G. Sinitsyna, Phys. At. Nucl. **67**, 1900 (2004)
[3] V.G. Sinitsyna Nuovo Cim. **19C**, 965 (1996)
[4] V. G. Sinitsyna, in Proc. of the 16th ECRS, Ed. by J. Medina (Univ. de Alcala, Spain, 1998), p. 383
[5] V.G. Sinitsyna, V.Y. Sinitsyna, J. Phys.: Conf. Ser. **718**, 052040 (2016)
[6] V.G. Sinitsyna, V.Y. Sinitsyna, Bull. Lebedev Phys. Inst. **40 (5)**, 113 (2013).
[7] T.-P.Li, Y.-Q. Ma Astrophys. J. **272** 317 (1983)
[8] S. Archambault et al., Astrophys. J. **779**, 150 (2013)
[9] J. Aleksić et al., Astrophys. J. **721**, 843 (2010)
[10] S. Kitamoto et al., Astron. Soc. Jpn. **47**, 233 (1995)
[11] M.H. van Kerkwijk et al., A&A. **314**, 521 (1996)
[12] M. van der Klis, J. M. Bonnet-Bidaud, A&A. **214**, 203 (1989).
[13] G. Manzo et al., A&A. **70**, 317 (1978).
[14] N.S. Singh et al., A&A **392**, 161 (2002).
[15] V.G. Sinitsyna, V.Yu. Sinitsyna, Astron. Lett. **44(3)**, 162 (2018)
[16] S. M. Matz, AIP Conf. Proc. **410**, 808 (1997)
[17] P. Goldoni, et al., A&A. **411**, L399 (2003)
[18] V.G. Sinitsyna,V.Yu. Sinitsyna, Astron. Lett. **40(2-3)**, 75 (2014)
[19] V.G. Sinitsyna et al, Advances in Space Research doi:10.1016/j.asr.2017.04.007 (2017)
[20] K.I.I. Koljonen, et al., MNRAS. **406**, 307 (2010)
[21] S. Heinz, R. Sunyaev, A&A. **390**, 751 (2002).
[22] V. Tudose et al., MNRAS **401**, 890 (2010).
[23] A.A. Abdo et al., Science **326**, 1512 (2009).
[24] A.A. Zdziarski et al., MNRAS. **421**, 2956 (2012)
[25] N. Sahakyan et al., Astrophys. J. **780**, 29 (2014)